Weakly Nonlinear Theory of Dynamic Fracture

Eran Bouchbinder, Ariel Livne, and Jay Fineberg
Racah Institute of Physics, Hebrew University of Jerusalem, Jerusalem 91904, Israel
(Received 30 July 2008; published 30 December 2008)

The common approach to crack dynamics, linear elastic fracture mechanics, assumes infinitesimal strains and predicts a $r^{-1/2}$ strain divergence at a crack tip. We extend this framework by deriving a weakly nonlinear fracture mechanics theory incorporating the leading nonlinear elastic corrections that must occur at high strains. This yields strain contributions "more divergent" than $r^{-1/2}$ at a finite distance from the tip and logarithmic corrections to the parabolic crack tip opening displacement. In addition, a dynamic length scale, associated with the nonlinear elastic zone, emerges naturally. The theory provides excellent agreement with recent near-tip measurements that cannot be described in the linear elastic fracture mechanics framework.

DOI: 10.1103/PhysRevLett.101.264302 PACS numbers: 46.50.+a, 62.20.mm, 62.25.Mn, 89.75.Kd

Understanding the dynamics of rapid cracks is a major challenge in condensed matter physics. For example, high velocity crack-tip instabilities [1,2] remain poorly understood from a fundamental point of view. Much of our understanding of how materials fail stems from linear elastic fracture mechanics (LEFM) [3], which assumes that materials are *linearly* elastic outside of a small zone where all nonlinear and dissipative processes occur. A central facet of LEFM is that strains diverge as $r^{-1/2}$ at a crack's tip and that this singularity dominates all other strain contributions in this region. Linear elasticity should be expected to break down before dissipative processes occur. The small size and rapid propagation velocity of the near-tip region of brittle cracks have, however, rendered quantitative measurements of the near-tip fields elusive.

In the companion Letter [4] such direct near-tip measurements of the displacement field $\boldsymbol{u}(\boldsymbol{r})$ were achieved for mode I cracks propagating at rapid velocities, v. Defining (r, θ) as coordinates moving with the crack tip, the propagation direction x is defined by $\theta = 0$ and the loading direction y by $\theta = \pi/2$. As predicted by LEFM, these experiments revealed that the crack tip opening profile, $u_y(r, \pm\pi)$, is parabolic beyond a velocity-dependent length scale $\delta(v)$. However, it was shown that although $u_x(r, \theta = 0)$ in this range also follows the functional form predicted by LEFM, its parameters are inconsistent with those described by $u_y(r, \pm\pi)$. Moreover, the strain component $\varepsilon_{yy}(r, 0) = \partial_y u_y(r, 0)$ was *wholly incompatible* with LEFM, indicating a "more divergent" behavior than $r^{-1/2}$. These puzzling discrepancies become increasingly severe as v increases.

In this Letter, we show that *all* of these puzzles can be quantitatively resolved by taking into account nonlinear corrections to linear elasticity, which *must* be relevant near the crack tip. This is achieved by perturbatively expanding the momentum balance equation for an elastic medium up to second order nonlinearities in the displacement gradients. The resulting theory provides a novel picture of the structure of the fields surrounding a crack tip, and may have implications for our understanding of crack dynamics.

Nonlinear material response at the large strains near a crack's tip motivates us to formulate a nonlinear elastic dynamic fracture problem under plane stress conditions. Consider the deformation field $\boldsymbol{\phi}$, which is assumed to be a continuous, differentiable, and invertible mapping between a reference configuration $\boldsymbol{x}$ and a deformed configuration $\boldsymbol{x}'$ such that $\boldsymbol{x}' = \boldsymbol{\phi}(\boldsymbol{x}) = \boldsymbol{x} + \boldsymbol{u}(\boldsymbol{x})$. The deformation gradient tensor $\boldsymbol{F}$ is defined as $\boldsymbol{F} = \boldsymbol{\nabla}\boldsymbol{\phi}$ or explicitly $F_{ij} = \delta_{ij} + \partial_j u_i$. The first Piola-Kirchhoff stress tensor $\boldsymbol{s}$, that is work-conjugate to the deformation gradient $\boldsymbol{F}$, is given as $\boldsymbol{s} = \partial_{\boldsymbol{F}} U(\boldsymbol{F})$, where $U(\boldsymbol{F})$ is the strain energy in the deformed configuration per unit volume in the reference configuration [5]. The momentum balance equation is

$$\boldsymbol{\nabla} \cdot \boldsymbol{s} = \rho \partial_{tt} \boldsymbol{\phi}, \tag{1}$$

where ρ is the reference mass density. Under steady-state propagation conditions we expect all of the fields to depend on x and t through the combination $x - vt$ and, therefore, $\partial_t = -v\partial_x$. The polar coordinate system that moves with the crack tip is related to the rest frame by $r = \sqrt{(x - vt)^2 + y^2}$ and $\theta = \tan^{-1}[y/(x - vt)]$. Thus, the traction-free boundary conditions on the crack faces are

$$s_{xy}(r, \theta = \pm\pi) = s_{yy}(r, \theta = \pm\pi) = 0. \tag{2}$$

To proceed, we note that in the measurement region of [4] the maximal strain levels are 0.2–0.35 (see below) as the velocity of propagation varied from $0.20c_s$ to $0.78c_s$, where $c_s = \sqrt{\mu/\rho}$ is the shear wave speed (μ is the shear modulus). These levels of strain motivate a perturbative approach where quadratic elastic nonlinearities must be taken into account. Higher order nonlinearities are neglected below, though they most probably become relevant as the crack velocity increases. We write the displacement field as

$$\boldsymbol{u}(r, \theta) \simeq \epsilon \boldsymbol{u}^{(1)}(r, \theta) + \epsilon^2 \boldsymbol{u}^{(2)}(r, \theta) + \mathcal{O}(\epsilon^3), \tag{3}$$

where ϵ quantifies the (dimensionless) magnitude of the strain. For a general $U(\boldsymbol{F})$, $\boldsymbol{s}$ and $\boldsymbol{\phi}$ can be expressed in terms of $\boldsymbol{u}$ of Eq. (3). Substituting these in Eqs. (1) and (2) one can perform a controlled expansion in orders of ϵ.

To make the derivation concrete, we need an explicit $U(\boldsymbol{F})$ that corresponds to the experiments of [4]. The polymer gel used in these experiments is well described by a plane stress incompressible neo-Hookean constitutive law [6], defined by the energy functional [7]

$$U(\boldsymbol{F}) = \frac{\mu}{2}[F_{ij}F_{ij} + \det(\boldsymbol{F})^{-2} - 3]. \tag{4}$$

Using this explicit $U(\boldsymbol{F})$, we derive the first order problem in ϵ

$$\mu\boldsymbol{\nabla}^2\boldsymbol{u}^{(1)} + 3\mu\boldsymbol{\nabla}(\boldsymbol{\nabla}\cdot\boldsymbol{u}^{(1)}) = \rho\ddot{\boldsymbol{u}}^{(1)}, \tag{5}$$

with the boundary conditions at $\theta = \pm\pi$

$$r^{-1}\partial_\theta u_x^{(1)} + \partial_r u_y^{(1)} = 0, \qquad 4r^{-1}\partial_\theta u_y^{(1)} + 2\partial_r u_x^{(1)} = 0. \tag{6}$$

This is a standard LEFM problem [3]. The near crack-tip (asymptotic) expansion of the steady-state solution for mode I symmetry is [3]

$$\epsilon u_x^{(1)}(r,\theta;v) = \frac{K_I\sqrt{r}}{4\mu\sqrt{2\pi}}\Omega_x(\theta;v) + \frac{\mathrm{Tr}\cos\theta}{3\mu} + \mathcal{O}(r^{3/2}),$$
$$\epsilon u_y^{(1)}(r,\theta;v) = \frac{K_I\sqrt{r}}{4\mu\sqrt{2\pi}}\Omega_y(\theta;v) - \frac{\mathrm{Tr}\sin\theta}{6\mu} + \mathcal{O}(r^{3/2}). \tag{7}$$

Here K_I is the mode I "stress intensity factor" and T is a constant known as the "T stress." Note that these parameters cannot be determined by the asymptotic analysis as they depend on the *global* crack problem. $\boldsymbol{\Omega}(\theta;v)$ is a known universal function [3,8]. ϵ in Eq. (3) can be now defined explicitly as $\epsilon \equiv K_I/[4\mu\sqrt{2\pi\ell(v)}]$, where $\ell(v)$ is a velocity-dependent length scale. $\ell(v)$ defines the scale where only the order ϵ and ϵ^2 problems are relevant. It is a *dynamic* length scale that marks the onset of deviations from a linear elastic constitutive behavior.

The solution of the order ϵ equation, i.e., Eq. (7), can be now used to derive the second order problem in ϵ. The form of the second order problem for an incompressible material is

$$\mu\boldsymbol{\nabla}^2\boldsymbol{u}^{(2)} + 3\mu\boldsymbol{\nabla}(\boldsymbol{\nabla}\cdot\boldsymbol{u}^{(2)}) + \frac{\mu\ell\boldsymbol{g}(\theta;v)}{r^2} = \rho\ddot{\boldsymbol{u}}^{(2)}, \tag{8}$$

where contributions proportional to T are neglected. The boundary conditions at $\theta = \pm\pi$ become

$$r^{-1}\partial_\theta u_x^{(2)} + \partial_r u_y^{(2)} = 4r^{-1}\partial_\theta u_y^{(2)} + 2\partial_r u_x^{(2)} + \frac{\kappa(v)\ell}{r} = 0. \tag{9}$$

Here $\boldsymbol{g}(\theta;v)$ and $\kappa(v)$ are known functions given in [8].

The problem posed by Eqs. (8) and (9) has the structure of an effective LEFM problem with a body force $\propto r^{-2}$ and a crack face force $\propto r^{-1}$. Note that Eqs. (8) and (9) are valid in the range $\sim\ell(v)$, where ϵ^2 is non-negligible with respect to ϵ, but higher order contributions are negligible. Since one cannot extrapolate the equations to smaller length scales, no real divergent behavior in the $r \to 0$ limit is implied. We stress that the structure of this problem is universal. Only $\boldsymbol{g}(\theta;v)$ and $\kappa(v)$ depend on the second order elastic constants resulting from expanding a *general* $U(\boldsymbol{F})$ to second order in ϵ. For example, the $\propto r^{-2}$ effective body force in Eq. (8) results from generic quadratic nonlinearities of the form $\partial(\partial u^{(1)}\partial u^{(1)})$.

We now focus on solving Eq. (8) with the boundary conditions of Eq. (9) for the explicit $\boldsymbol{g}(\theta;v)$ and $\kappa(v)$ derived from Eq. (4) [8]. Our strategy is to look for a particular solution of the inhomogeneous Eq. (8) *without* satisfying the boundary conditions of Eq. (9) and then to add to it a solution of the corresponding homogeneous equation that makes the overall solution consistent with the boundary conditions. We find that the inhomogeneous solution, $\boldsymbol{\Upsilon}(\theta;v)$, is r independent. The homogeneous solution is obtained using a standard approach [3] by noting that the second boundary condition of Eq. (9) requires that its first spatial derivative scales as r^{-1}. The second order solution for mode I symmetry is

$$\epsilon^2 u_x^{(2)}(r,\theta;v) = \left(\frac{K_I}{4\mu\sqrt{2\pi}}\right)^2\Bigg[A\log r + \frac{A}{2}\log\left(1 - \frac{v^2\sin^2\theta}{c_d^2}\right) + B\alpha_s\log r + \frac{B\alpha_s}{2}\log\left(1 - \frac{v^2\sin^2\theta}{c_s^2}\right) + \Upsilon_x(\theta;v)\Bigg],$$
$$\epsilon^2 u_y^{(2)}(r,\theta;v) = \left(\frac{K_I}{4\mu\sqrt{2\pi}}\right)^2[-A\alpha_d\theta_d - B\theta_s + \Upsilon_y(\theta;v)],$$
$$\tan\theta_{d,s} = \alpha_{d,s}\tan\theta, \quad \alpha_{d,s}^2 \equiv 1 - v^2/c_{d,s}^2, \tag{10}$$

where $A = [2\alpha_s B - 4\partial_\theta\Upsilon_y(\pi;v) - \kappa(v)]/(2 - 4\alpha_d^2)$ [cf. Eq. (9)] and c_d is the dilatational wave speed. $c_d = 2c_s$ in an incompressible material under plane stress conditions.

The analytic form of $\boldsymbol{\Upsilon}(\theta;v)$ depends mainly on $\boldsymbol{g}(\theta;v)$. The latter can be represented as

$$g_x(\theta;v) \simeq \sum_{n=1}^{N(v)} a_n(v)\cos(n\theta), \quad g_y(\theta;v) \simeq \sum_{n=1}^{N(v)} b_n(v)\sin(n\theta). \tag{11}$$

For $v = 0$ we have $N(0) = 3$ and the representation is *exact*, while for higher velocities it provides analytic approximations with whatever accuracy needed. For $v \simeq 0.8c_s$ only seven terms provide a representation that can be regarded exact for any practical purpose [8]. $\boldsymbol{\Upsilon}(\theta;v)$ is then obtained in the form

$$\Upsilon_x(\theta;v) \simeq \sum_{n=1}^{N(v)} c_n(v)\cos(n\theta), \quad \Upsilon_y(\theta;v) \simeq \sum_{n=1}^{N(v)} d_n(v)\sin(n\theta), \tag{12}$$

where the unknown coefficients are determined by solving a linear set of equations [8]. A striking feature of Eq. (10) is that they lead to strain contributions that vary as r^{-1}, which are "more singular" than the $r^{-1/2}$ strains predicted by LEFM.

We now show that the second order solution of Eq. (10) entirely resolves the discrepancies raised by trying to interpret the experimental data of [4] in the framework of LEFM. The complete second order asymptotic solution, Eqs. (3), (7), and (10), contains three parameters (K_I, T, and B) that cannot be determined from the asymptotic solution and therefore must be extracted from the experimental data.

These parameters were chosen such that Eqs. (3), (7), and (10) properly describe the measured $u_x(r, 0)$. Examples for $v/c_s = 0.20$, 0.53, and 0.78 are provided in Fig. 1 (top). With K_I, T, and B at hand, we can now test the theory's predictions for $\varepsilon_{yy}(r, 0)$ with no adjustable free parameters. The corresponding results are compared with both the measured data [4] and LEFM predictions in Fig. 1 (bottom). In general, the agreement with the experimental data is excellent. These results demonstrate the importance of the predicted r^{-1} strain terms near the crack tip. ℓ is estimated as the scale where the largest strain component reaches values of 0.10–0.15. For the data presented in Fig. 1(a), $\varepsilon_{yy} > \varepsilon_{xx}$, where $\varepsilon_{xx} = \partial_x u_x$ is obtained by differentiating u_x. Thus, ℓ can be read off of the bottom panel to be ~0.5–1 mm. Similar estimates can be obtained for every v, though not always does $\varepsilon_{yy} > \varepsilon_{xx}$, e.g., Fig. 1(c).

For $v = 0.53c_s$ [Fig. 1(b)] the theory still agrees well with the measurements, although some deviations near the tip are observed. These deviations signal that higher order corrections may be needed, though second order nonlinearities still seem to provide the dominant correction to LEFM. For higher velocities, it is not clear, *a priori*, that second order nonlinearities are sufficient to describe the data. In fact, the strain component $\varepsilon_{xx}(r, 0)$ for $v = 0.78c_s$ reaches a value of ~0.35 in Fig. 1(c), suggesting that higher order nonlinearities may be important. Nevertheless, the second order theory avoids a fundamental failure of LEFM; at high velocities ($v > 0.73c_s$ for an incompressible material) LEFM predicts [dashed line in Fig. 1(c)] that the contribution proportional to K_I in $\varepsilon_{yy}(r, 0)$ [derived from Eq. (7)] becomes *negative*. This implies that $\varepsilon_{yy}(r, 0)$ *decreases* as the crack tip is approached and becomes *compressive*. This is surprising, as material points straddling $y = 0$ must be separated from one another to precipitate fracture. Thus, the second order nonlinear solution (solid line), though applied beyond its range of validity, already induces a qualitative change in the character of the strain. This is a striking manifestation of the breakdown of LEFM, demonstrating that elastic nonlinearities are generally unavoidable, especially as high crack velocities are reached. The results of Figs. 1(a)–1(c) both provide compelling evidence in favor of the developed theory and highlight inherent limitations of LEFM. We note that $\ell(v)$ increases with increasing v, reaching values in the millimeter scale at very high v.

Our results indicate that the widely accepted assumption of "K dominance" of LEFM, i.e., that there is always a region where the $r^{-1/2}$ strain term dominates all other contributions, is violated here. The results presented in Fig. 1 explicitly demonstrate that quadratic nonlinearities become important in the same region where a non-negligible T stress exists. As elastic nonlinearities intervene before the $r^{-1/2}$ term dominates the strain fields, the contributions of *both* of these terms must be taken into account as one approaches the crack tip. Since values of the T stress and of B are system specific, this observation is valid for the specific experimental system under study. They do indicate that the assumption of "K dominance" is not always valid.

An additional puzzle raised in [4] was that although the form of both $u_x(r, 0)$ and the crack tip opening displacement (CTOD) agreed with LEFM, the respective derived values of K_I differed by about 20%, cf. Fig. 3a in [4]. This

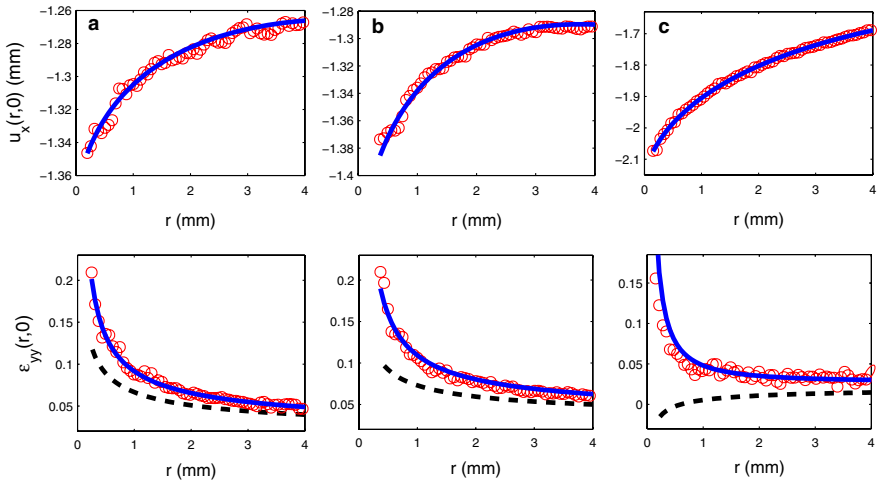

FIG. 1 (color online). Top: Measured $u_x(r, 0)$ (circles) fitted to the x component of Eq. (3) (solid line) for (a) $v = 0.20c_s$ with $K_I = 1070$ Pa$\sqrt{m}$, $T = -3150$ Pa, and $B = 18$; (b) $v = 0.53c_s$ with $K_I = 1250$ Pa$\sqrt{m}$, $T = -6200$ Pa, and $B = 7.3$; (c) $v = 0.78c_s$ with $K_I = 980$ Pa$\sqrt{m}$, $T = -6900$ Pa, and $B = 26$. Bottom: Corresponding measurements of $\varepsilon_{yy}(r, 0) = \partial_y u_y(r, 0)$ (circles) compared to the theoretical nonlinear solution [cf. Eq. (3)] *with no adjustable parameters* (solid lines); K_I, T, and B are taken from the fit of $u_x(r, 0)$. LEFM predictions (analysis as in [4]) were added for comparison (dashed lines).

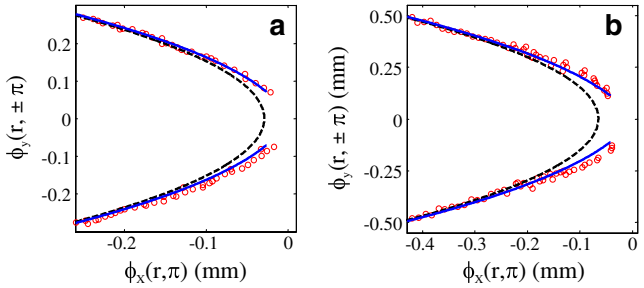

FIG. 2 (color online). Measured crack-tip profiles [$\phi_y(r, \pm\pi)$ vs $\phi_x(r, \pi)$] (circles). Shown are the parabolic LEFM best fit (dashed line) and the profiles predicted by the second order nonlinear corrections (solid line). (a) $v = 0.2c_s$ and (b) $v = 0.53c_s$. T and B are as in Fig. 1. In contrast to the ~20% discrepancy in values of K_I obtained in [4], the respective values $K_I = 1170$ Pa$\sqrt{m}$ and $K_I = 1300$ Pa$\sqrt{m}$ correspond to within 9% and 4%, respectively, of K_I obtained from $u_x(r, 0)$ using the nonlinear theory, cf. Fig. 1.

puzzle is resolved by the theory as follows. The form of the CTOD is given by $\phi_y(r, \pm\pi)$ as a function of the distance, $\phi_x(r, \pi)$, from the crack tip in the moving (laboratory) frame. Substituting $\theta = \pi$ into Eqs. (3), (7), and (10), the nonlinear theory predicts that the CTOD remains parabolic, where the $\log(r)$ term in $\phi_x(r, \pi)$ is negligible compared to r. This occurs at the *same* scale $\ell(v)$ at which nonlinear corrections are essential to describe the strain at $\theta = 0$, cf. Fig. 1. Quantitatively, the parabolic CTOD can be described with K_I values that differ from those describing $u_x(r, 0)$ by only a few percent with the *same* values of T and B (cf. Fig. 1). This small K_I variation is possibly related to subleading nonlinear corrections associated with the T stress and will be addressed elsewhere.

Let us now consider the CTOD in the near vicinity of the crack tip, i.e., when r is further reduced. Equations (10) predict the existence of log terms in $\phi_x(r, \theta)$. These terms, which are negligible at $\theta = \pi$ on a scale $\ell(v)$, must become noticeable at smaller scales. Although this region is formally beyond the range of validity of the expansion of Eq. (3), we would still expect the existence of a CTOD contribution proportional to $\log r$ to be observable. We test this prediction in Fig. 2 by comparing the measured small-scale CTOD to both the parabolic LEFM form and the second order nonlinear solution with no adjustable parameters. We find that these log terms, whose coefficients were determined at a scale $\ell(v)$, capture the initial deviation from the parabolic CTOD at $\theta = \pm\pi$ to a surprising degree of accuracy. This result lends further independent support to the validity of Eq. (10).

In summary, we have shown that the second order solution presented in Eq. (10) resolves in a self-consistent way all of the puzzles that were highlighted in [4]. As this is accomplished without dissipation, this result suggests that elastic nonlinearities are the dominant correction to LEFM at these scales. This solution is universal in the sense that its generic properties are independent of geometry, loading conditions, and material parameters. We would entirely expect that *any* material subjected to the enormous deformations that surround the tip of a crack must experience *at least* quadratic elastic nonlinearities, prior to the onset of the irreversible deformation that leads to failure. Our results show that these deformations, which are the vehicle for transmitting breaking stresses to crack tips, must be significantly different from the LEFM description, especially at high v.

One may ask why we should not consider still higher order elastic nonlinearities. We surmise that quadratic elastic nonlinearities may be special, as they mark the emergence of a dynamic length scale $\ell(v)$ that characterizes a region where material properties—like local wave speeds, local response times, and anisotropy—become *deformation dependent*. This line of thought seems consistent with the observations of Ref. [9]. As supporting evidence for this view, we note that the geometry-independent wavelength of crack path oscillations discussed in [2,10] seems to correlate with the millimeter scale $\ell(v)$ at high v. Therefore, our results may have implications for understanding crack-tip instabilities.

This research was supported by Grant No. 57/07 of the Israel Science Foundation. E. B. acknowledges support from the Horowitz Center for Complexity Science and the Lady Davis Trust.

[1] J. Fineberg and M. Marder, Phys. Rep. **313**, 1 (1999).
[2] A. Livne, O. Ben-David, and J. Fineberg, Phys. Rev. Lett. **98**, 124301 (2007).
[3] L. B. Freund, *Dynamic Fracture Mechanics* (Cambridge University Press, Cambridge, England, 1998).
[4] A. Livne, E. Bouchbinder, and J. Fineberg, preceding Letter, Phys. Rev. Lett. **101**, 264301 (2008).
[5] A detailed discussion on the different stress and strain measures can be found in G. A. Holzapfel, *Nonlinear Solid Mechanics* (Wiley, Chichester, 2000).
[6] A. Livne, G. Cohen, and J. Fineberg, Phys. Rev. Lett. **94**, 224301 (2005).
[7] J. K. Knowles and E. Sternberg, J. Elast. **13**, 257 (1983); G. Ravichandran and W. G. Knauss, Int. J. Fract. **39**, 235 (1989).
[8] See EPAPS Document No. E-PRLTAO-102-011902 for explicit expressions. For more information on EPAPS, see http://www.aip.org/pubservs/epaps.html.
[9] M. J. Buehler, F. F. Abraham, and H. Gao, Nature (London) **426**, 141 (2003); M. J. Buehler and H. Gao, Nature (London) **439**, 307 (2006).
[10] E. Bouchbinder and I. Procaccia, Phys. Rev. Lett. **98**, 124302 (2007).